

# Quantum Statistical Effects on Warm Dark Matter and the Mass Constraint from the Cosmic Large Scale Structure

ZHIJIAN ZHANG<sup>1</sup> AND WEIKANG LIN<sup>1</sup>

<sup>1</sup>*South-Western Institute For Astronomy Research, Yunnan University, Kunming 650500, Yunnan, P. R. China*

## ABSTRACT

The suppression of small-scale matter power spectrum is a distinct feature of Warm Dark Matter (WDM), which permits a constraint on the WDM mass from galaxy surveys. In the thermal relic WDM scenario, quantum statistical effects are not manifest. In a unified framework, we investigate the quantum statistical effects for a fermion case with a degenerate pressure and a boson case with a Bose-Einstein condensation (BEC). Compared to the thermal relic case, the degenerate fermion case only slightly lowers the mass bound while the boson case with a high initial BEC fraction ( $\gtrsim 90\%$ ) significantly lowers it. On the other hand, the BEC fraction drops during the relativistic-to-nonrelativistic transition and completely disappears if the initial fraction is below  $\sim 64\%$ . Given the rising interest in resolving the late-time galaxy-scale problems with boson condensation, a question is posed on how a high initial BEC fraction can be dynamically created so that a DM condensed component remains today.

## 1. INTRODUCTION

A wide range of cosmological and astronomical phenomena from galaxy scales (Zwicky 1933; Smith 1936; van de Hulst et al. 1957; Clowe et al. 2006; Lin & Ishak 2016) to large scales (Dark Energy Survey Collaboration et al. 2018; Hikage et al. 2019; Joudaki et al. 2018; Ade & others (Planck Collaboration) 2020) point to the existence of dark matter (DM). However, little is known about dark matter except that they are around five times in mass as baryons and are highly nonrelativistic at the time of recombination (i.e., cold). Here, we assume that dark matter is some unknown particles.

An important parameter of DM is the particle mass, which is related to almost all aspects of the DM study such as model buildings, early-universe production mechanisms, and direct and indirect searches. The cosmic large-scale structure (LSS) has been a powerful probe of DM properties, especially the “warmness” of DM. The DM early-time thermal motion smooths out the structures and prevents gravitational growth at small scales. In the thermal relic scenario, WDM became a free stream when they were still relativistic. Matching the current DM energy density requires that lighter DM be warmer. So, the nondetection of the suppression of the matter power spectrum puts a lower bound of the WDM mass (Colombi et al. 1996), which is currently of a few keV (Iršič et al. 2024).

Such a constraint is not absolute but depends on the assumption of the DM production mechanism (Bhupal Dev et al. 2014). In particular, while a fermion WDM is assumed in the usual thermal relic scenario, quantum statistical effects only play a minor role. When the WDM number density is larger than that in the thermal relic scenario, quantum statistical effects begin to be significant. For the fermion case, a degenerate pressure is added on top of the thermal pressure (Bar et al. 2021; Carena et al. 2022). For the boson case, a Bose-Einstein condensation (BEC) component appears (Madsen 1992) and can affect the cosmic background evolution and structure formation (Fukuyama & Morikawa 2006; Harko 2011; Chavanis 2012).

Given the importance of the WDM mass constraint and the growing interest in quantum effects on galaxy and cosmological scales, in this work, we investigate how quantum statistical effects impact the mass constraint from LSS. From the view of conservation of specific entropy, we analyze the evolution of quantum statistical effects during the relativistic-to-nonrelativistic transition (RNRT) and their impacts on RNRT and LSS. In particular, compared previous works on cosmological DM condensation (Fukuyama & Morikawa 2006; Harko 2011), we focus on how the BEC fraction evolves during RNRT and the effects on the WDM mass constraint from LSS. The scenario considered in this work serves as a minimum extension to the thermal relic WDM that considers both a degenerate fermion case and a boson case with a BEC component. We dub it the quantum Warm Dark Matter (qWDM).

We adopt the units  $G = c = k_B = 1$ .

## 2. ANALYSIS

We consider a single-species ideal-gas DM that has an equilibrium phase-space distribution,

$$f(p; T, \mu) = \frac{g}{2\pi^2 h^3} \frac{p^2}{\exp[(\sqrt{p^2 + m^2} - \mu)/T] \pm 1}, \quad (1)$$

with a mass  $m$ , intrinsic degree of freedom  $g$ , temperature  $T$ , chemical potential  $\mu$ . In the denominator,  $+1$  is for fermion and  $-1$  for boson. Note that this DM temperature  $T$  is different from the standard-sector temperature. In this work, we do not assume any early thermal contact between DM and the standard model (SM) and thus DM remains hidden.<sup>1</sup> Since we assume DM has an equilibrium phase-space distribution instead of being a free stream, it requires some DM-DM interaction to keep DM in equilibrium at least in the early time (Egana-Ugrinovic et al. 2021). We take  $g = 2$  for the fermion case and  $g = 1$  for the boson case, but the conclusions obtained in this work can be readily generalized to cases with a higher  $g$ .

We define the following two dimensionless variables,

$$x \equiv \frac{m}{T}, \quad (2)$$

$$\Delta \equiv \frac{\mu - m}{T}. \quad (3)$$

Then,  $x$  is the mass-to-temperature ratio and  $\Delta$  is the effective chemical potential-to-temperature. We call  $\mu - m$  the effective chemical potential for the following reason. In the relativistic limit, the mass  $m$  can be ignored. In the non-relativistic limit, the distribution Eq. (1) reduces to the non-relativistic form, from which we can identify  $\mu - m$  as the nonrelativistic chemical potential.

From Eq. (1), we calculate the physical particle number density  $n$ , energy density  $\rho$ , pressure  $P$  as well as entropy density  $s$  for given temperature and chemical potential; see appendix A. Some important results for  $n$ ,  $\rho$ ,  $P$ , and  $s/n$  in the relativistic and nonrelativistic limits are summarized in Table 1. Those limits are useful for obtaining the relations between the initial and final values of dynamical variables and verifying our numerical solutions of the qWDM background evolution.

The parameter  $\Delta$  is an important parameter in determining the degree of quantum statistical effects. The system is called classical when  $\Delta \rightarrow -\infty$  and Eq. (1) reduces to the Boltzmann-Maxwell distribution. For the fermion case, the degenerate pressure begins to play a role when  $\Delta > 0$  and the system is highly degenerate when  $\Delta \rightarrow \infty$ . For the boson case, a Bose-Einstein condensation (BEC) can take place

when  $\Delta = 0$ . In that case, we define the fraction of the BEC component as

$$r \equiv \frac{n_{\text{BEC}}}{n_{\text{tot}}}, \quad (4)$$

where  $n_{\text{BEC}}$  is the particle number density of qWDM in the BEC state and  $n_{\text{tot}} = n + n_{\text{BEC}}$  is the total qWDM number density. We assume that there is no internal energy state and the BEC component of DM condenses into the zero-momentum state so that the total energy density is

$$\rho_{\text{tot}} = \rho + mn_{\text{BEC}}. \quad (5)$$

Note that  $n_{\text{tot}} = n$  and  $\rho_{\text{tot}} = \rho$  for the fermion case.

The background (homogeneous level) evolution of the qWDM thermodynamical variables, e.g.,  $\rho(a)$  and  $P(a)$ , is solved assuming the conservation of comoving particle number and the conservation of specific entropy, that is,<sup>2</sup>

$$n_{\text{tot}} a^3 = \text{constant}, \quad (6)$$

$$s/n_{\text{tot}} = \text{constant}, \quad (7)$$

where  $a$  is the scale factor. See Appendix A for the details of the numerical calculation of the background evolution.

### 2.1. The DM energy density today

For the fermion case, the initial temperature and chemical potential determine the thermal WDM number density. For the boson case with a BEC component, the initial chemical potential vanishes, but the initial fraction of the BEC component  $r_i$  is a free parameter. For both cases, the total DM energy density today is the product of the total number density and the mass. It can be shown that the DM energy density fraction today is given by

$$\Omega_{\text{dm}} h^2 = \frac{g}{2} \beta(\Delta_i, r_i) \frac{m}{94 \text{ eV}} \frac{\alpha^3}{4/11}, \quad (8)$$

where

$$\beta(\Delta_i, r_i) \equiv \frac{J_3^\mp(\Delta_i)}{(1 - r_i) J_3^-(0)}, \quad (9)$$

$\alpha \equiv \frac{T_0}{T_\gamma}$  with  $T_0 \equiv \lim_{a \rightarrow 0} aT$  and  $T_\gamma^0$  is the photon temperature today. Please see Table 1 for the definition of the  $J$ 's functions. Now, the superscript “ $-$ ” is for fermion and “ $+$ ” for boson. Note that, while we matched the form of Eq. (8) to that of Eq. (6) in Colombi et al. (1996), the  $\beta$  here is determined by the initial effective chemical potential-to-temperature ratio and the initial fraction of BEC component

<sup>1</sup> It is more suitable to call our scenario the “Hidden Dark Matter” (Chen & Tye 2006), which is more generalized. We adopted the term WDM to better highlight the quantum statistical effects compared to the thermal relic scenario.

<sup>2</sup> Note that, with the particle number conservation, the qWDM evolution obtained based on the conservation of specific entropy is equivalent to that obtained based on the energy conservation. However, using the conservation of specific entropy allows us to see clearly how the quantum statistical effects evolve, as we will discuss.

instead of an arbitrary factor in the momentum distribution. For the same initial temperature, Both a higher degree of degeneracy for the fermion case and a higher BEC fraction for the boson case give a higher  $\beta$  factor and a higher DM density today. However,  $\alpha$  is not directly related to an observable and we shall replace it in Eq. (8) with the RNRT scale factor, which predominantly determines the suppression scale of the matter power spectrum.

## 2.2. The relativistic-to-nonrelativistic transition

After we solve for the background evolution, the adiabatic sound speed is calculated by

$$c_s = \sqrt{\frac{dP/da}{d\rho_{\text{tot}}/da}}. \quad (10)$$

In general, qWDM starts with a relativistic phase where  $c_s$  equals  $1/\sqrt{3}$  and then transitions to a nonrelativistic phase where it drops as  $1/a$ . We define the transition scale factor  $a_{\text{nr}}$  by the following asymptotic behavior of  $c_s$  in the nonrelativistic limit,

$$c_s \xrightarrow{\text{nonrelativistic}} \frac{1}{\sqrt{3}} \frac{a_{\text{nr}}}{a}. \quad (11)$$

That is,  $a_{\text{nr}}$  is the scale factor at which the nonrelativistic sound speed would increase to  $1/\sqrt{3}$  if it kept increasing inverse-linearly with  $a$  when going back in time.

Different quantum statistics have distinct effects on  $a_{\text{nr}}$ . The fiducial case corresponding to (but somewhat different from) the thermal relic WDM scenario is a fermion case with a vanishing initial chemical potential and  $g = 2$ . This case has only a small difference from the classical case on the value of  $a_{\text{nr}}$  for the same initial conditions (Lin et al. 2023). We show the evolution of  $c_s$  for the classical case by the orange curve in Figure 1.

For the fermion case with a positive initial  $\Delta$  (denoted as  $\Delta_i$ ), the degenerate pressure postpones RNRT with a larger  $a_{\text{nr}}$  compared to the classical case. The larger  $\Delta_i$ , the larger  $a_{\text{nr}}$ . The reason is the following. In the presence of the degenerate pressure, the condition  $m \gg T$  (or  $x \gg 1$ ) is no longer sufficient to define the nonrelativistic phase as it would be in the classical case. If the degenerate pressure is high enough, a large fraction of DM particles can still occupy relativistic momentum states. Mathematically, only when  $x \gg \Delta$  will the momenta of most particles be smaller than the mass and Eq. (1) be approximated by a nonrelativistic form. Therefore, the nonrelativistic limit requires both  $x \gg 1$  and  $x \gg \Delta$ , that is, in addition, the particle mass needs to be much larger than the effective chemical potential. During the relativistic phase,  $x$  increases linearly with  $a$ , but  $\Delta$  remains a constant. Only when  $x$  increases to be larger than  $\Delta$  will DM enter the nonrelativistic phase. As a result, the higher the initial degree of degeneracy (i.e., the

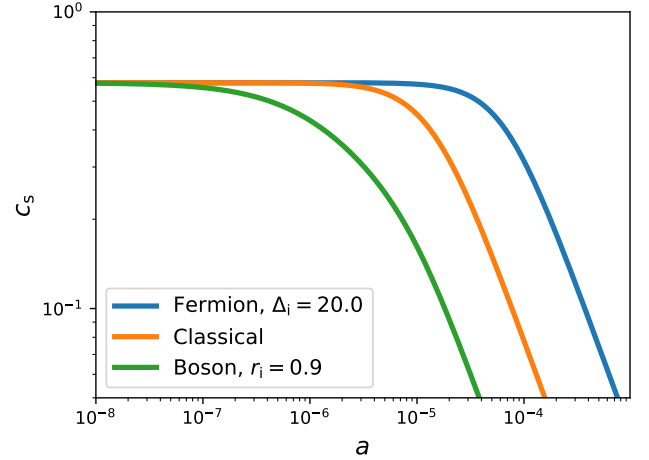


**Figure 1.** Effects from quantum statistics on the adiabatic sound speed. The degenerate pressure postpones the relativistic-to-nonrelativistic transition for the fermion case, while a BEC component for the boson case expedites it. The same initial value of  $x/a$  is applied.

larger  $\Delta_i$ ), the later the transition. Such an effect is shown by the blue curve in Figure 1.

For the boson case with a fraction of the BEC component, an opposite effect takes place and the transition is advanced compared to the classical case. This is because now  $x \ll 1$  is not the criteria for the relativistic phase. When  $x \ll 1$  with the presence of a BEC component, the total energy density is,

$$\rho_{\text{tot}} = \rho + mn_{\text{BEC}} = \rho \left( 1 + \frac{rx}{1-r} \frac{J_3^+(0)}{J_4^+(0)} \right), \quad (12)$$

where both  $J_3^+(0)$  and  $J_4^+(0)$  are of the order of unity. Meanwhile,  $P = \rho/3$  is still satisfied for  $x \ll 1$ . When  $x \sim (1-r)/r$ , the term  $mn_{\text{BEC}}$  is comparable to  $\rho$  and the pressure. This estimate breaks down at small  $r$  values where higher order terms in  $x$  are needed. Numerical analyses suggest that such an estimate is good for  $r \sim 1$  and that  $x \ll (1-r)$  is a good criterion for the relativistic phase for all  $r > 0$ . Then, once  $x$  increases to  $(1-r)$ , qWDM already begins to enter the nonrelativistic phase. Therefore, the larger  $r_i$ , the earlier the RNRT.

For all cases, the transition scale is proportional to the initial value of  $a/x$ , that is,

$$a_{\text{nr}} = C_{\text{cs}}(\Delta_i, r_i) \frac{T_0}{m}. \quad (13)$$

The coefficient  $C_{\text{cs}}$  depends on the initial degree of degeneracy for the fermion case and the initial BEC fraction for the boson case. It can be derived analytically. This is done by first substituting the nonrelativistic forms of  $\rho$  and  $P$  (see Table 1) into Eq. (10) to relate  $c_s$  and  $x$  in the nonrelativistic

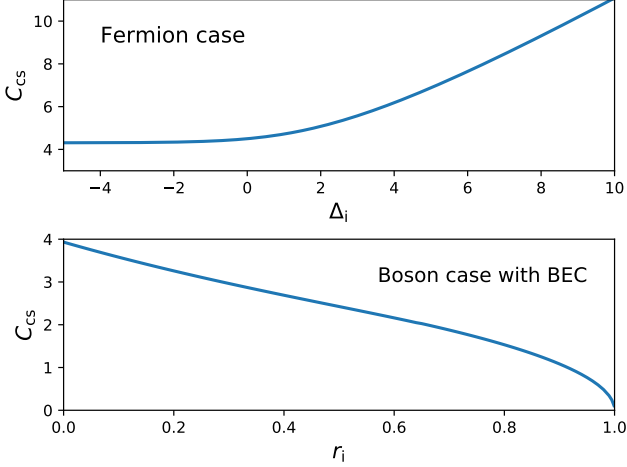


**Figure 2.** The effect of quantum statistics on the coefficient  $C_{cs}$  defined in Eq.(13). The larger  $C_{cs}$ , the later the relativistic-to-nonrelativistic transition for a given initial mass-to-temperature ratio.

phase. Then, the asymptotic evolution of  $x$  at the nonrelativistic phase can be derived by matching the initial and the final comoving particle density. As a result, it can be shown that,

$$C_{cs} = \left(\frac{5}{3}\right)^{1/2} \frac{(1-r_i)^{5/6} (J_3^\mp(\Delta_i))^{1/3} (J_{5/2}^\mp(\Delta_f))^{1/2}}{(1-r_i)^{1/3} (J_{3/2}^\mp(\Delta_f))^{5/6}}. \quad (14)$$

The larger  $C_{cs}$ , the later the transition. We show  $C_{cs}$  as function of  $\Delta_i$  and  $r_i$  in Figure 2. By combining Eqs. (8) and (13), we relate the DM energy fraction to the transition scale factor which reads

$$\Omega_{\text{dm}} h^2 = 0.12 \times \frac{g}{2} \gamma(\Delta_i, r_i) \left(\frac{m}{m_0}\right)^4 \left(\frac{a_{\text{nr}}}{\hat{a}_{\text{nr}}}\right)^3, \quad (15)$$

where  $m_0 = 0.97 \text{ keV}$ ,  $\hat{a}_{\text{nr}} = 1.8 \times 10^{-7}$  and

$$\begin{aligned} \gamma(\Delta_i, r_i) &= \beta(\Delta_i, r_i) \left(\frac{C_{cs}^0}{C_{cs}}\right)^3 \\ &= \left(\frac{J_{3/2}^\mp(\Delta_f)}{(1-r_i)J_{3/2}^\mp(\Delta_f^0)}\right)^{5/2} \left(\frac{J_{5/2}^\mp(\Delta_f^0)}{J_{5/2}^\mp(\Delta_f)}\right)^{3/2}, \end{aligned} \quad (16)$$

where  $C_{cs}^0$  and  $\Delta_f^0$  are the values of  $C_{cs}$  and  $\Delta_f$  in the fiducial case (i.e., a fermion case with  $\Delta_i = 0$ ). The value of  $\hat{a}_{\text{nr}}$  is motivated by the discussion on the suppression scale in the next section.

### 2.3. The suppression scale of matter power spectrum

To obtain the theoretical prediction of the (comoving) suppression scale of the matter power spectrum, we first estimate

it by the qWDM sound horizon scale,

$$\begin{aligned} \ell_s^{\text{est}} &= \int c_s d\eta = \int \frac{c_s}{a^2 H} da \\ &\simeq \frac{1}{\sqrt{3}} \left( \int_0^{a_{\text{nr}}} \frac{da}{a^2 H} + \int_{a_{\text{nr}}}^{a_{\text{eq}}} \frac{a_{\text{nr}} da}{a^3 H} + \int_{a_{\text{eq}}}^1 \frac{a_{\text{nr}} da}{a^3 H} \right) \\ &\simeq 234 \text{ Mpc} \times \frac{a_{\text{nr}}}{a_{\text{eq}}} \left(1 - \frac{1}{3} \ln \frac{a_{\text{nr}}}{a_{\text{eq}}}\right). \end{aligned} \quad (17)$$

We then follow the procedure in Lin et al. (2023) to implement the adiabatic sound speed in the linear perturbation and the public Boltzmann code CAMB (Lewis et al. 2000) and numerically calculate the matter power spectrum today. We define the suppression scale  $\ell_s$  as the scale where the matter power spectrum in the qWDM case is half of that in the CDM case, that is,

$$\frac{P_{\text{qWDM}}(\ell_s)}{P_{\text{CDM}}(\ell_s)} = \frac{1}{2}. \quad (18)$$

The fact that the estimation  $\ell_s^{\text{est}}$  is only  $\sim 2$  times smaller than the numerical  $\ell_s$  motivates us to parameterize  $\ell_s$  as

$$\ell_s = 1 \text{ Mpc} \times \frac{a_{\text{nr}}}{A} \left(1 - B \ln \frac{a_{\text{nr}}}{A}\right). \quad (19)$$

We find that  $A = \hat{a}_{\text{nr}} = 1.8 \times 10^{-7}$  and  $B = 0.16$  make Eq. (19) fit the numerical results well.<sup>3</sup> For a given qWDM mass,  $a_{\text{nr}}$  can be inferred from Eq. (15), which is put in Eq. (19) to give  $\ell_s$ . Despite the different physical settings, the  $\ell_s$  inferred for a given mass with  $\Delta_i = 0$  and  $g = 2$  is only a factor of  $\sim 1.5$  different compared to that in the free-streaming thermal relic WDM scenario provided in other works such as Bode et al. (2001); Hansen et al. (2002); Viel et al. (2013).

To make the connection between the qWDM mass and  $\ell_s$  clearer, we combine Eqs. (15) and (19) to obtain

$$\Omega_{\text{dm}} h^2 = 0.12 \times \frac{g}{2} \gamma(\Delta_i, r_i) \left(\frac{m}{m_0}\right)^4 \left[ K_{\text{inv}} \left(\frac{\ell_s}{1 \text{ Mpc}}\right) \right]^3, \quad (20)$$

where  $K_{\text{inv}}$  is the inverse function of

$$K(y) = y(1 - 0.16 \ln y). \quad (21)$$

Importantly, since LSS constrains  $\ell_s$ , from Eq. (20) we can see that the quantum statistical effects on the constraint of the WDM mass are reflected in  $\gamma$ . Then, from Eq. (16), there are the two dominant factors that affect  $\gamma$  and hence the mass constraint: (1)  $\beta$ , that is the ratio of number density between the qWDM case and the thermal relic WDM case; (2)  $C_{cs}$ , that determines the time of RNRT.

<sup>3</sup> Besides  $a_{\text{nr}}$  that dominantly determines the suppression scale, different quantum statistics also make the transition width somewhat different; see Lin et al. (2023). While we ignored such a small difference, including it does not qualitatively change our conclusions.

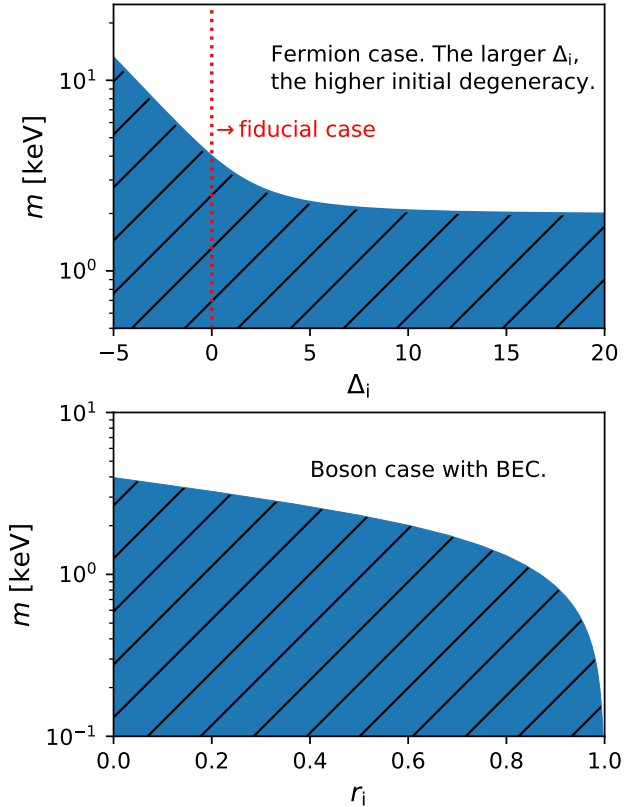


**Figure 3.** Estimated DM mass constraints from the Ly $\alpha$  forest. Hatched parameter regions are excluded. Top: the fermion case. The mass lower bound is stronger at the classical limit but becomes constant at the highly degenerate limit. The red-dotted vertical line corresponds to the fiducial case. Bottom: the boson case with a fraction of the BEC component. The mass lower bound is significantly lowered at a high BEC fraction.

### 3. THE MASS CONSTRAINTS

It is now ready to investigate the effects of quantum statistics on the WDM mass constraint from the LSS. So far, the suppression on the small-scale matter power spectrum has not been observed and it thus puts a lower limit on the WDM mass. Recently, a strong constraint of  $\ell_s$  is given in Iršič et al. (2024) that the matter power spectrum cannot drop more than 5% at the wavenumber of  $14.35 h\text{Mpc}^{-1}$ . This corresponds to  $\ell_s < 0.135 h^{-1}\text{Mpc}$ .<sup>4</sup> We take  $h = 0.674$  and  $\Omega_{\text{dm}} h^2 = 0.12$  (Ade & others (Planck Collaboration) 2020). According to Eq. (20), the upper bound of  $\ell_s$  is then translated into a lower bound of the WDM mass which depends on the degree of quantum statistics. In Figure 3 we show the constraints of the qWDM mass as a function of  $\Delta_i$  for the fermion case and  $r_i$  for the boson case.

<sup>4</sup> We have used  $\left(\frac{P_{\text{WDM}}}{P_{\text{CDM}}}\right)^{1/2} \simeq (1 + (\alpha k)^{2\mu})^{-5/\mu}$  (Bode et al. 2001) with  $\mu = 1.12$  (Viel et al. 2005).

For the fiducial case, the mass is constrained to be  $m > 4.0$  keV. This constraint is somewhat different from  $m > 5.7$  keV given in Iršič et al. (2024) because we assume WDM keeps an equilibrium phase-space distribution instead of being a free stream; also see Egana-Ugrinovic et al. (2021). The classical case with  $\Delta_i \ll -1$  makes the mass lower bound stronger (i.e., higher). This is because the DM particle number is smaller in the classical case than in the fiducial case and then the  $\beta$  factor is smaller. Meanwhile, the  $C_{\text{cs}}$  factor is similar as long as  $\Delta_i < 0$ . These result in a smaller  $\gamma$  factor in Eq. (20) and a higher mass bound in the classical case compared to the fiducial case.

For the fermion case with the presence of degenerate pressure, the mass constraint is only slightly lowered than the fiducial case. Two effects occur that almost cancel out each other and leave the mass constraint almost unchanged. First, DM is denser compared to the fiducial case, which raises the  $\beta$  factor in Eq. (8) and tends to lower the mass constraint. But, as discussed in Sec. 2.2, RNRT is postponed due to the degenerate pressure so that  $C_{\text{cs}}$  is also larger. Both  $\beta$  and  $C_{\text{cs}}^3$  have the same asymptotic dependence on  $\Delta_i$ , i.e.,  $\propto \Delta_i^3$  when  $\Delta_i \gg 1$ . As a result, the  $\gamma$  factor becomes a constant and the qWDM mass lower bound becomes independent on  $\Delta_i$  at the highly degenerate limit. Despite the different analyses here, the conclusion that fermionic degenerate pressure only slightly lowers the WDM mass constraint is consistent with other works; see (Bar et al. 2021; Carena et al. 2022).

For the boson case with a BEC component, the mass constraint can be significantly lowered with a high BEC fraction. Similar to the fermion case, DM is denser compared to the fiducial case. However, different from the fermion case, now the transition is advanced. The net effect results in a larger  $\gamma$  factor and a lowered mass bound. At a high BEC fraction, the WDM mass bound can be arbitrarily low. This clearly shows that DM constituted of condensation, such as that of the fuzzy DM (Ji & Sin 1994; Hu et al. 2000), can avoid the WDM mass bound. However, we can see from the lower panel of Figure 3 that a high initial BEC fraction ( $r_i \gtrsim 0.9$ ) is needed to lower the mass bound significantly.

Eventually at the low mass region for the boson case with a very high or even a 100% BEC component, the WDM mass will be restricted due to the “quantum pressure” (Chavanis 2012; Iršič et al. 2017; Dalal & Kravtsov 2022), the study of which is out of the scope of this work.

### 4. REMARKS ON QUANTUM STATISTICAL EFFECTS DURING THE TRANSITION

The degree of quantum statistical effects drops during RNRT, which can be readily seen with the conservation of specific entropy. When  $\Delta_i < 0$ , both the fermion and boson cases share similar behavior and reduce to the classical case in the  $\Delta_i \ll -1$  limit (Lin et al. 2023), so we discuss here



the situations where  $\Delta_i > 0$  for the fermion case and  $r_i > 0$  (with  $\Delta_i = 0$ ) for the boson case.

For the fermion case,  $\Delta$  drops from one constant  $\Delta_i$  in the relativistic phase to another constant  $\Delta_f$  in the nonrelativistic phase. Thus, the degenerate pressure can only appear today if it appeared in the early universe. The drop of  $\Delta$  is a result of the conservation of specific entropy. In both the relativistic and nonrelativistic phases, the specific entropy  $s/n$  is a monotonic decreasing function only of  $\Delta$ . On the other hand, for a given  $\Delta$ ,  $s/n$  is smaller in the nonrelativistic phase than in the relativistic phase. Thus, to keep the specific entropy constant during RNRT,  $\Delta$  must decrease. By equating the relativistic and nonrelativistic limits of  $s/n$  [see Eq. (A9)], it can be shown that in the highly degenerate limit (i.e.,  $\Delta \rightarrow \infty$ ),  $\Delta$  drops to half of its initial value, i.e.,  $\Delta_f = \frac{1}{2}\Delta_i$ . So, if qWDM was initially in a highly degenerate state, it remains a highly degenerate state today.

For the boson case with an initial BEC component, i.e.,  $\Delta_i = 0$  and  $r_i > 0$ , the BEC fraction drops from one constant at the relativistic phase to another constant at the nonrelativistic phase. This is also a result of the conservation of specific entropy. Recall that it is  $s/n_{\text{tot}} = (1-r)s/n$  that remains a constant. We know that when  $\Delta = 0$ ,  $s/n$  decreases during the transition. Thus,  $r$  needs to decrease to keep  $s/n_{\text{tot}}$  constant. Therefore, qWDM can have a BEC component today only if it started with some BEC component. This agrees with the expectation in Fukuyama & Morikawa (2006). Quantitatively, by equating the initial and final specific entropy, one can show that the final BEC fraction  $r_f$  is related to the initial  $r_i$  by

$$r_f = 1 - \frac{1 - r_i}{1 - r_i^{\text{cr}}}, \quad (22)$$

with

$$r_i^{\text{cr}} = 1 - \frac{5J_{5/2}^+(0)J_3^+(0)}{4J_{3/2}^+(0)J_4^+(0)} \simeq 0.6435 \quad (23)$$

being a critical initial BEC fraction. We have  $r_f > 0$  if  $r_i > r_i^{\text{cr}}$ . Thus, *only when the initial BEC fraction is higher than  $\sim 64\%$  will a BEC component remain today.* This conclusion holds even if the boson DM has some internal energy states. This is because Eq. (22) is obtained based on the conservation of particle number and specific entropy, and the condensed component in some internal states does not contribute to the system's entropy.

When  $r_i < r_i^{\text{cr}}$ , the BEC fraction drops to 0 at some point during RNRT, and then  $\Delta$  drops from 0 to a negative value until the nonrelativistic phase. On the other hand, if  $r_i \rightarrow 1$ , we also have  $r_f \rightarrow 1$  from Eq. (22). Therefore, if qWDM started with a highly condensed state, it remains a highly condensed state today.

## 5. SUMMARY AND CONCLUSION

In this work, we have studied the quantum statistical effects of a single-species WDM on the early-time background evolution of the density and pressure, cosmic structure growth, and the mass constraint from the Lyman- $\alpha$  forest. We have considered situations where the system is degenerate for a fermion DM or where a BEC component appears for a boson DM. We have paid special attention to the change of the quantum statistical effects during RNRT, which affects the WDM sound horizon and the suppression scale of the matter power spectrum.

When quantum statistical effects are considered, two factors predominantly affect the constraint on the WDM mass from LSS. One is the qWDM number density compared to the thermal relic WDM case. The other is the time of the qWDM relativistic-to-nonrelativistic transition. Situations with a higher qWDM number density and an earlier transition make the mass lower bound weaker (i.e., the bound is lower). In both the degenerate fermion case and the boson case with a BEC component, the number density is higher than in the thermal relic WDM case. For the fermion case, the degenerate pressure postpones RNRT. The net effect is the DM mass constraint is only slightly lower in the degenerate fermion case compared to that in the thermal relic WDM case. On the other hand, the boson case with a BEC component advances RNRT. As a result, the DM mass lower bound can be significantly relaxed. However, a large initial BEC fraction ( $n_{\text{BEC}}/n_{\text{tot}} \gtrsim 90\%$ ) is required to substantially weaken the mass lower bound.

The degree of degeneracy for the fermion case and the BEC fraction for the boson case decrease during RNRT, both of which are results of the conservation of specific entropy. In particular, for the boson case, the BEC fraction drops to zero unless the initial BEC fraction is higher than about 64%. Small-scale problems have motivated proposals that involve boson DM with a completely or partially condensed state, but dynamically generating a BEC component does not achieve such a high initial fraction (Madsen 1992). This does not constitute immediate trouble to scenarios where the boson DM somehow directly starts with a completely condensed state as is what is taken for, e.g., axion DM (Preskill et al. 1983; Abbott & Sikivie 1983; Dine & Fischler 1983), Fuzzy DM (Ji & Sin 1994; Hu et al. 2000) and others (Fukuyama & Morikawa 2006). However, it poses a question on how to generate a high DM BEC fraction dynamically. To avoid the above constraint, one way is the BEC state is generated during the nonrelativistic phase of DM. Another way is that small-scale BEC can be somehow formed during gravitational collapse. A caveat in this work is that we assume qWDM is an ideal gas in an equilibrium phase-space distribution so that the background evolution can be established in a parameterized way. This implicitly puts a constraint on the type and the strength of the self-interaction. Considering

more general self-interaction may result in different evolution (Harko 2011; Guth et al. 2015).

1 W. L. thanks Vid Iršič for answering the questions about  
 2 the unit of wavenumber used in the Lyman- $\alpha$  forest flux  
 3 power spectrum, Xingang Chen and Amol Upadh for  
 4 useful feedback. W. L. acknowledges that this work  
 5 is supported by the ‘‘Science & Technology Champion  
 6 Project’’ (202005AB160002) and the ‘‘Top Team Project’’  
 7 (202305AT350002), both funded by the ‘‘Yunnan Revitaliza-  
 8 tion Talent Support Program.’’ This work is also supported by  
 9 the ‘‘Yunnan General Grant’’ (202401AT070489).

## APPENDIX

### A. METHODS

#### A.1. Thermodynamical variables and their relativistic and the nonrelativistic limits

To obtain the quantum statistical effects, we first calculate the background evolution of the qWDM density and pressure, then derive the adiabatic sound speed and implement it into the cosmic linear perturbation. Here, we highlight the key steps of the procedure used in Lin et al. (2023). With the momentum distribution given in Eq. (1), the qWDM number density, energy density, and pressure can be calculated with

$$n = \int_0^\infty f(p) dp, \quad (\text{A1})$$

$$\rho = \int_0^\infty f(p) \sqrt{p^2 + m^2} dp, \quad (\text{A2})$$

$$P = \int_0^\infty \frac{f(p) p^2}{\sqrt{p^2 + m^2}} dp. \quad (\text{A3})$$

By defining the mass-to-temperature ratio  $x \equiv m/T$  and the effective chemical potential-to-temperature ratio  $\Delta \equiv (\mu - m)/T$ , the above can be cast into following forms,

$$n = \frac{n_*}{x^3} \mathcal{N} \quad \text{with} \quad \mathcal{N}(x, \Delta) = \int_0^\infty \frac{dz z^2}{\exp(\sqrt{z^2 + x^2} - x - \Delta) \pm 1}, \quad (\text{A4})$$

$$\rho = \frac{n_* m}{x^4} \mathcal{R} \quad \text{with} \quad \mathcal{R}(x, \Delta) = \int_0^\infty \frac{dz z^2 \sqrt{z^2 + x^2}}{\exp(\sqrt{z^2 + x^2} - x - \Delta) \pm 1} \quad (\text{A5})$$

$$P = \frac{n_* m}{x^4} \mathcal{P} \quad \text{with} \quad \mathcal{P}(x, \Delta) = \frac{1}{3} \int_0^\infty \frac{dz z^4 / \sqrt{z^2 + x^2}}{\exp(\sqrt{z^2 + x^2} - x - \Delta) \pm 1}, \quad (\text{A6})$$

where  $n_* = \frac{gm^3}{2\pi^2 \hbar^3}$ . The relativistic and nonrelativistic limits of Eqs. (A4)-(A6) can be calculated analytically which we give in Table 1. Note that the condition for the nonrelativistic limit is  $x \gg 1$  and  $x \gg \Delta$  as we explained.

From Euler’s theorem on homogeneous functions, the entropy of an ideal gas is given by  $TS = (U + VP - \mu N)$  for given volume  $V$ , energy  $U$  (including the rest-energy), and particle number  $N$ . Dividing it by  $V$  and  $T$ , we obtain the entropy density which reads,

$$s = \frac{\rho + P - \mu n}{T}. \quad (\text{A7})$$

Then, with Eqs. (A4)-(A6) the specific entropy is then given by

$$\frac{s}{n} = \frac{\mathcal{R}(x, \Delta) + \mathcal{P}(x, \Delta)}{\mathcal{N}(x, \Delta)} - x - \Delta. \quad (\text{A8})$$

Note that while Eq. (A8) still holds for the boson case with a BEC component with  $n$  being the density of the thermal component, the correct specific entropy that conserves is  $s/n_{\text{tot}} = (1 - r)s/n$ . We show the dependence of  $s/n$  on  $x$  and  $\Delta$  in Figure 4. For

	The relativistic limit, $x \ll 1$	The nonrelativistic limit, $x \gg 1$ and $x \gg \Delta$
	$\mathcal{N} = J_3^\mp(\Delta) + 2xJ_2^\mp(\Delta) + \mathcal{O}(x^2)$ $\mathcal{R} = J_4^\mp(\Delta) + 3xJ_3^\mp(\Delta) + \mathcal{O}(x^2)$ $\mathcal{P} = \frac{1}{3}\mathcal{R} + \mathcal{O}(x^2)$ $s/n = \frac{4J_4^\mp(\Delta)}{3J_3^\mp(\Delta)} - \Delta + \mathcal{O}(x^2)$	$\mathcal{N} = \frac{1}{2}(2x)^{3/2} \left( J_{3/2}^\mp(\Delta) + \frac{5}{4x} J_{5/2}^\mp(\Delta) + \mathcal{O}\left(\frac{1}{x^2}\right) \right)$ $\mathcal{R} = \frac{1}{2}x \cdot (2x)^{3/2} \left( J_{3/2}^\mp(\Delta) + \frac{9}{4x} J_{5/2}^\mp(\Delta) + \mathcal{O}\left(\frac{1}{x^2}\right) \right)$ $\mathcal{P} = \frac{1}{3}(2x)^{3/2} \left( J_{5/2}^\mp(\Delta) + \mathcal{O}\left(\frac{1}{x}\right) \right)$ $s/n = \frac{5J_{5/2}^\mp(\Delta)}{3J_{3/2}^\mp(\Delta)} - \Delta + \mathcal{O}\left(\frac{1}{x^2}\right)$
$\Delta \leq 0$	$J_s^\mp(\Delta) = \Gamma(s) f_s^\mp(\Delta) \exp(\Delta)$	
$\Delta > 0$ fermion	$J_s^-(\Delta) = \frac{1}{s}\Delta^s + \sum_{k=1}^{k \leq \frac{s}{2}} A_s^k J_{2k}^-(0) \Delta^{s-2k} + (-1)^{s-1} J_s^-(-\Delta)$  where $A_s^k = \frac{2 \times (s-1)!}{(2k-1)!(s-2k)!}$	$J_{3/2}^-(\Delta) = \frac{2}{3}\Delta^{3/2} + \frac{\sqrt{\pi}}{2} \sum_{n=1}^{\infty} \frac{(-1)^{n-1}}{n^{3/2}} \times$ $\left( \operatorname{erfi}(\sqrt{n\Delta}) e^{-n\Delta} + \operatorname{erfc}(\sqrt{n\Delta}) e^{n\Delta} \right)$  $J_{5/2}^-(\Delta) = \frac{2}{5}\Delta^{5/2} + \frac{\pi^2}{4}\Delta^{1/2} + \frac{3\sqrt{\pi}}{4} \sum_{n=1}^{\infty} \frac{(-1)^n}{n^{5/2}} \times$ $\left( \operatorname{erfi}(\sqrt{n\Delta}) e^{-n\Delta} - \operatorname{erfc}(\sqrt{n\Delta}) e^{n\Delta} \right)$

**Table 1.** Summary of the relativistic and the non-relativistic limits of the characteristic functions of thermal number density ( $n = \frac{gm^3}{2\pi^2\hbar^3} \frac{1}{x^3} \mathcal{N}$ ), energy density ( $\rho = \frac{gm^4}{2\pi^2\hbar^3} \frac{1}{x^4} \mathcal{R}$ ), pressure ( $p = \frac{gm^4}{2\pi^2\hbar^3} \frac{1}{x^4} \mathcal{P}$ ), and specific entropy  $s/n$  ( $n$  is the thermal number density only). The relativistic (non-relativistic) limit is defined as  $x \ll 1$  ( $x \gg 1$  and  $x \gg \Delta$ ). The function  $f_s^\mp$  is defined as  $f_s^\mp(\Delta) \equiv \sum_{n=0}^{\infty} \frac{(\mp 1)^n}{(n+1)^s} \exp(n\Delta) = \Phi(e^{\mp\Delta}, s, 1)$ , where now  $-$  is for fermion,  $+$  for boson, and  $\Phi$  is the Lerch transcendent. The functions  $\operatorname{erfi}$  and  $\operatorname{erfc}$  are the complementary and imaginary error functions. For the boson case with a BEC component, the above equations apply to the thermal component with  $\Delta = 0$ . The integration forms of the  $J$ 's functions are defined as  $J_s^\mp(\Delta) \equiv \int_0^\infty \frac{z^{s-1} dz}{\exp(z-\Delta) \pm 1}$ . Some important properties are  $\frac{d}{d\Delta} J_s^\mp(\Delta) = (s-1)J_{s-1}^\mp(\Delta)$ . Note that the subscript  $s$  is an integer or half-integer not to be confused with the entropy density.

a given  $\Delta$ , the value of  $n/s$  is a constant in the relativistic limit and is a smaller constant in the nonrelativistic limit. The large  $|\Delta|$  behaviors of the relativistic and nonrelativistic limits of  $s/n$  are useful and given by (positive  $\Delta$  only applies to the fermion case),

$$s/n = \begin{cases} \frac{4J_4^\mp(\Delta)}{3J_3^\mp(\Delta)} - \Delta & (\text{for } x \ll 1) \\ \frac{5J_{5/2}^\mp(\Delta)}{3J_{3/2}^\mp(\Delta)} - \Delta & (\text{for } x \gg 1 \text{ \& } x \gg \Delta) \end{cases} = \begin{cases} \frac{\pi^2}{\Delta} & \text{for } x \ll 1 \text{ \& } \Delta \gg 1, \text{ relativistic and degenerate,} \\ -\Delta + 4 & \text{for } x \ll 1 \text{ \& } \Delta \ll -1, \text{ relativistic and classical,} \\ \frac{\pi^2}{2\Delta} & \text{for } x \gg \Delta \gg 1, \text{ nonrelativistic and degenerate,} \\ -\Delta + 5/2 & \text{for } x \gg 1 \text{ \& } \Delta \ll -1, \text{ nonrelativistic and classical.} \end{cases} \quad (\text{A9})$$

## A.2. The background evolution

The two independent dynamical variables are  $x$  and  $\Delta$  ( $x$  and  $r$  for the boson case with  $\Delta = 0$ ), whose background evolution is derived using the conservation of the comoving particle number and the conservation of the specific entropy (concerning the total particle number), that is

$$d(n_{\text{tot}} a^3) = 0, \quad (\text{A10})$$

$$d(s/n_{\text{tot}}) = 0. \quad (\text{A11})$$



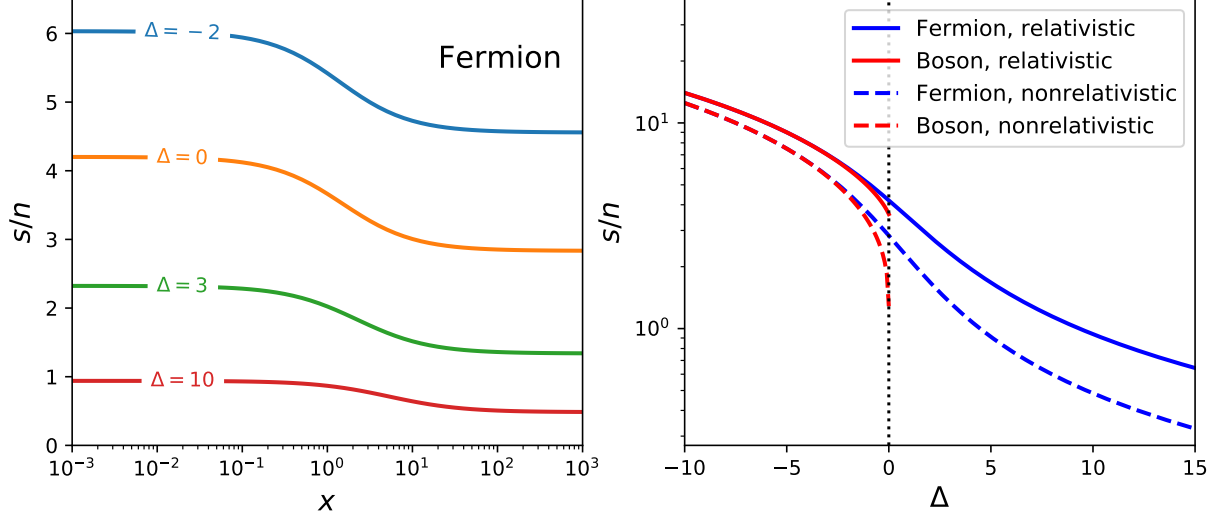


**Figure 4.** The dependence of thermal specific entropy  $s/n$  on the mass-to-temperature ratio  $x$  and the effective chemical potential-temperature ratio  $\Delta$ . Left: curves of  $s/n$  as a function of  $x$  for some fixed  $\Delta$ 's for the fermion case. For a given  $\Delta$ ,  $s/n$  drops from a constant in the relativistic limit to another constant in the nonrelativistic limit. Right: curves of  $s/n$  as a function of  $\Delta$  in the relativistic limit (solid) and in the nonrelativistic limit (dashed). The blue curves are for fermion and the red curves are for boson. Note that, for the boson case, the specific entropy concerning the total particle number is  $s/n_{\text{tot}} = (1 - r)s/n$ .

The above conditions set up the differential equations for  $x$  and  $\Delta$  as functions of the scale factor  $a$ , which, for the fermion case and the boson case without condensation, read

$$\begin{pmatrix} d \ln x \\ d \Delta \end{pmatrix} = \begin{pmatrix} 1 - \frac{x}{3\mathcal{N}}\mathcal{N}_x & -\frac{1}{3\mathcal{N}}\mathcal{N}_\Delta \\ \frac{x}{\mathcal{N}}\xi_x - \frac{x\xi}{\mathcal{N}^2}\mathcal{N}_x - x & \frac{1}{\mathcal{N}}\xi_\Delta - \frac{\xi}{\mathcal{N}^2}\mathcal{N}_\Delta - 1 \end{pmatrix}^{-1} \begin{pmatrix} d \ln a \\ 0 \end{pmatrix}, \quad (\text{A12})$$

where  $\xi = \mathcal{R} + \mathcal{P}$  and the subscripts denote partial derivatives (e.g.,  $\xi_x \equiv \frac{\partial \xi}{\partial x}$ ). For the boson case with a BEC component, qWDM begins with  $\Delta = 0$  and  $r > 0$ . Then, Eqs. (A10) and (A11) reduce to a differential equation for  $x$ ,

$$\frac{d \ln x}{d \ln a} = \frac{3(x\mathcal{N} - \xi)}{2x\mathcal{N} - x^2\mathcal{N}_x - 3\xi + x\xi_x} \Big|_{\Delta=0}. \quad (\text{A13})$$

We integrate the above equation to find  $x(a)$ , which is then substituted into  $(1 - r)s/n = \text{constant}$  to give  $r(a)$ . If the initial BEC fraction is  $r_i > r_{\text{cr}}$  [see Eq. (23)], the integration of Eq. (A13) proceeds until  $r = 0$ , and we continue to solve Eq. (A12) with the initial value of  $x$  given by that at  $r = 0$ . Otherwise, the integration of Eq. (A13) proceeds until  $a = 1$ .

The initial conditions are described as the following. For both the fermion and boson cases, the value of  $x/a$  is a constant in the early universe. Thus, we specify the value of  $x/a$  in the relativistic limit as the first initial condition. We call  $T_0/m \equiv \lim_{a \rightarrow 0} a/x$  the initial ‘‘warmness’’ of qWDM. The second initial condition is treated differently for two possibilities. For the fermion case and the boson case without a BEC component, the value of  $\Delta$  is a constant in the early universe. In this case, we specify  $\Delta$  in the relativistic limit ( $\Delta_i$ ) as the second initial condition. For the boson case with  $\Delta = 0$ , a BEC component appears. The BEC fraction  $r$  is constant in the early universe. In that case, we use  $r$  in the relativistic limit ( $r_i$ ) as the second initial condition. That is, the initial conditions are specified by the set of  $(x_i/a_i, \Delta_i)$ , except for the boson case with  $\Delta_i = 0$  where they are specified by  $(x_i/a_i, r_i)$ .

With the background evolution of  $x$  and  $\Delta$  obtained above, we substitute them into Eqs. (A4)-(A6) to get the background evolution of the number density, energy density and pressure of qWDM. We assume the qWDM perturbation is an adiabatic process with the adiabatic sound speed calculated by Eq. (10). With a finite equation of state and a finite adiabatic sound speed, the qWDM linear perturbation equations are modified compared to the cold DM case and read (Ma & Bertschinger 1995),

$$\delta'_{\text{qWDM}} = -kq_{\text{qWDM}} - (1 + w_{\text{qWDM}})h'_s/2 + 3\mathcal{H}(w_{\text{qWDM}} - c_s^2)\delta_{\text{qWDM}}, \quad (\text{A14})$$

$$q'_{\text{qWDM}} = (3w_{\text{qWDM}} - 1)\mathcal{H}q_{\text{qWDM}} + kc_s^2\delta_{\text{qWDM}}, \quad (\text{A15})$$

where  $\delta_{\text{qWDM}}$  and  $q_{\text{qWDM}}$  are the qWDM overdensity and heat flux,  $'$  denotes the derivative with respect to the conformal time,  $w_{\text{qWDM}} \equiv \frac{P}{\rho_{\text{tot}}}$ ,  $\mathcal{H}$  is the conformal Hubble parameter, and  $h_s$  and  $\eta_s$  are the two synchronous gauge gravitational variables (Ma & Bertschinger 1995). We have omitted the pressure anisotropy in Eq. (A15) since we assume qWDM has an equilibrium phase-space distribution that is isotropic. We implement the above linear perturbation into the public code CAMB (Lewis et al. 2000) to calculate the linear matter power spectrum and determine the suppression scale using Eq. (18).

## REFERENCES

- Abbott, L. F., & Sikivie, P. 1983, *Phys. Lett. B*, 120, 133, doi: [10.1016/0370-2693\(83\)90638-X](https://doi.org/10.1016/0370-2693(83)90638-X)
- Ade, P. A. R., & others (Planck Collaboration). 2020, *A&A*, 641, A6, doi: [10.1051/0004-6361/201833910](https://doi.org/10.1051/0004-6361/201833910)
- Bar, N., Blas, D., Blum, K., & Kim, H. 2021, *Phys. Rev. D*, 104, 043021, doi: [10.1103/PhysRevD.104.043021](https://doi.org/10.1103/PhysRevD.104.043021)
- Bhupal Dev, P. S., Mazumdar, A., & Qutub, S. 2014, *Front. in Phys.*, 2, 26, doi: [10.3389/fphy.2014.00026](https://doi.org/10.3389/fphy.2014.00026)
- Bode, P., Ostriker, J. P., & Turok, N. 2001, *The Astrophysical Journal*, 556, 93, doi: [10.1086/321541](https://doi.org/10.1086/321541)
- Carena, M., Coyle, N. M., Li, Y.-Y., McDermott, S. D., & Tsai, Y. 2022, *Phys. Rev. D*, 106, 083016, doi: [10.1103/PhysRevD.106.083016](https://doi.org/10.1103/PhysRevD.106.083016)
- Chavanis, P. H. 2012, *A&A*, 537, A127, doi: [10.1051/0004-6361/201116905](https://doi.org/10.1051/0004-6361/201116905)
- Chen, X., & Tye, S.-H. H. 2006, *JCAP*, 6, 011, doi: [10.1088/1475-7516/2006/06/011](https://doi.org/10.1088/1475-7516/2006/06/011)
- Clowe, D., Bradač, M., Gonzalez, A. H., et al. 2006, *ApJL*, 648, L109, doi: [10.1086/508162](https://doi.org/10.1086/508162)
- Colombi, S., Dodelson, S., & Widrow, L. M. 1996, *ApJ*, 458, 1, doi: [10.1086/176788](https://doi.org/10.1086/176788)
- Dalal, N., & Kravtsov, A. 2022, *Phys. Rev. D*, 106, 063517, doi: [10.1103/PhysRevD.106.063517](https://doi.org/10.1103/PhysRevD.106.063517)
- Dark Energy Survey Collaboration, Abbott, T. M. C., et al. 2018, *PhRvD*, 98, 043526, doi: [10.1103/PhysRevD.98.043526](https://doi.org/10.1103/PhysRevD.98.043526)
- Dine, M., & Fischler, W. 1983, *Phys. Lett. B*, 120, 137, doi: [10.1016/0370-2693\(83\)90639-1](https://doi.org/10.1016/0370-2693(83)90639-1)
- Egana-Ugrinovic, D., Essig, R., Gift, D., & LoVerde, M. 2021, *JCAP*, 05, 013, doi: [10.1088/1475-7516/2021/05/013](https://doi.org/10.1088/1475-7516/2021/05/013)
- Fukuyama, T., & Morikawa, M. 2006, *J. Phys. Conf. Ser.*, 31, 139, doi: [10.1088/1742-6596/31/1/023](https://doi.org/10.1088/1742-6596/31/1/023)
- Guth, A. H., Hertzberg, M. P., & Prescod-Weinstein, C. 2015, *Phys. Rev. D*, 92, 103513, doi: [10.1103/PhysRevD.92.103513](https://doi.org/10.1103/PhysRevD.92.103513)
- Hansen, S. H., Lesgourgues, J., Pastor, S., & Silk, J. 2002, *Mon. Not. Roy. Astron. Soc.*, 333, 544, doi: [10.1046/j.1365-8711.2002.05410.x](https://doi.org/10.1046/j.1365-8711.2002.05410.x)
- Harko, T. 2011, *Phys. Rev. D*, 83, 123515, doi: [10.1103/PhysRevD.83.123515](https://doi.org/10.1103/PhysRevD.83.123515)
- Hikage, C., et al. 2019, *Publications of the Astronomical Society of Japan*, 22, doi: [10.1093/pasj/psz010](https://doi.org/10.1093/pasj/psz010)
- Hu, W., Barkana, R., & Gruzinov, A. 2000, *Phys. Rev. Lett.*, 85, 1158, doi: [10.1103/PhysRevLett.85.1158](https://doi.org/10.1103/PhysRevLett.85.1158)
- Iršič, V., Viel, M., Haehnelt, M. G., Bolton, J. S., & Becker, G. D. 2017, *Phys. Rev. Lett.*, 119, 031302, doi: [10.1103/PhysRevLett.119.031302](https://doi.org/10.1103/PhysRevLett.119.031302)
- Iršič, V., et al. 2024, *Phys. Rev. D*, 109, 043511, doi: [10.1103/PhysRevD.109.043511](https://doi.org/10.1103/PhysRevD.109.043511)
- Ji, S. U., & Sin, S. J. 1994, *Phys. Rev. D*, 50, 3655, doi: [10.1103/PhysRevD.50.3655](https://doi.org/10.1103/PhysRevD.50.3655)
- Joudaki, S., et al. 2018, *MNRAS*, 474, 4894, doi: [10.1093/mnras/stx2820](https://doi.org/10.1093/mnras/stx2820)
- Lewis, A., Challinor, A., & Lasenby, A. 2000, *The Astrophysical Journal*, 538, 473, doi: [10.1086/309179](https://doi.org/10.1086/309179)
- Lin, W., Chen, X., Ganjoo, H., Hou, L., & Mack, K. J. 2023, <https://arxiv.org/abs/2305.08943>
- Lin, W., & Ishak, M. 2016, *JCAP*, 10, 025, doi: [10.1088/1475-7516/2016/10/025](https://doi.org/10.1088/1475-7516/2016/10/025)
- Ma, C.-P., & Bertschinger, E. 1995, *ApJ*, 455, 7, doi: [10.1086/176550](https://doi.org/10.1086/176550)
- Madsen, J. 1992, *Phys. Rev. Lett.*, 69, 571, doi: [10.1103/PhysRevLett.69.571](https://doi.org/10.1103/PhysRevLett.69.571)
- Preskill, J., Wise, M. B., & Wilczek, F. 1983, *Phys. Lett. B*, 120, 127, doi: [10.1016/0370-2693\(83\)90637-8](https://doi.org/10.1016/0370-2693(83)90637-8)
- Smith, S. 1936, *The Astrophysical Journal*, 83, 23
- van de Hulst, H. C., Raimond, E., & van Woerden, H. 1957, *Bull. Astron. Inst. Netherlands*, 14, 1
- Viel, M., Becker, G. D., Bolton, J. S., & Haehnelt, M. G. 2013, *Phys. Rev. D*, 88, 043502, doi: [10.1103/PhysRevD.88.043502](https://doi.org/10.1103/PhysRevD.88.043502)
- Viel, M., Lesgourgues, J., Haehnelt, M. G., Matarrese, S., & Riotto, A. 2005, *PhRvD*, 71, 063534, doi: [10.1103/PhysRevD.71.063534](https://doi.org/10.1103/PhysRevD.71.063534)
- Zwicky, F. 1933, *Helv. Phys. Acta*, 6, 15